

## Chromospheric activity on the late-type star V1355 Ori using Lijiang 1.8-m and 2.4-m telescopes

Qing-Feng Pi<sup>1,2,3</sup>, Li-Yun Zhang<sup>1,2</sup>, Liang Chang<sup>2,4</sup>, Xian-Ming Han<sup>1,5</sup>, Hong-Peng Lu<sup>1,2</sup>,  
Xi-Liang Zhang<sup>2,4</sup> and Dai-Mei Wang<sup>1,2</sup>

<sup>1</sup> College of Physics/Department of Physics and Astronomy, Guizhou University, Guiyang 550025, China;  
piqingfeng@126.com, liy\_zhang@hotmail.com

<sup>2</sup> Key Laboratory for the Structure and Evolution of Celestial Objects, Chinese Academy of Sciences, Kunming 650011, China

<sup>3</sup> Mingde College, Guizhou University, Guiyang 550025, China

<sup>4</sup> Yunnan Observatories, Chinese Academy of Sciences, Kunming 650011, China

<sup>5</sup> Dept. of Physics and Astronomy, Butler University, Indianapolis, IN 46208, USA

Received 2015 December 23; accepted 2016 May 26

**Abstract** We obtained new high-resolution spectra using the Lijiang 1.8-m and 2.4-m telescopes to investigate the chromospheric activities of V1355 Ori as indicated in the behaviors of Ca II H&K, H $\delta$ , H $\gamma$ , H $\beta$ , Na I D<sub>1</sub>, D<sub>2</sub>, H $\alpha$  and Ca II infrared triplet (IRT) lines. The observed spectra show obvious emissions above the continuum in Ca II H&K lines, absorptions in the H $\delta$ , H $\gamma$ , H $\beta$  and Na I D<sub>1</sub>, D<sub>2</sub> lines, variable behavior (filled-in absorption, partial emission with a core absorption component or emission above the continuum) in the H $\alpha$  line, and weak self-reversal emissions in the strong filled-in absorptions of the Ca II IRT lines. We used a spectral subtraction technique to analyze our data. The results show no excess emission in the H $\delta$  and H $\gamma$  lines, very weak excess emissions in the Na I D<sub>1</sub>, D<sub>2</sub> lines, excess emission in the H $\beta$  line, clear excess emission in the H $\alpha$  line, and excess emissions in the Ca II IRT lines. The value of the ratio of EW<sub>8542</sub>/EW<sub>8498</sub> is in the range 0.9 to 1.7, which implies that chromospheric activity might have been caused by plage events. The value of the ratio  $E_{H\alpha}/E_{H\beta}$  is above 3, indicating that the Balmer lines would arise from prominence-like material. We also found time variations in light curves associated with equivalent widths of chromospheric activity lines in the Na I D<sub>1</sub>, D<sub>2</sub>, Ca II IRT and H $\alpha$  lines in particular. These phenomena can be explained by plage events, which are consistent with the behavior of chromospheric activity indicators.

**Key words:** stars: chromosphere — stars: activity — stars: individual (V1355 Ori)

### 1 INTRODUCTION

V1355 Ori (BD -00 1147, HD 291095, K0-2 IV, 3.82 days) is a single-line spectroscopic RS CVn binary (Strassmeier et al. 1999, 2000; Strassmeier 2000; Savanov & Strassmeier 2008; Eker et al. 2008; etc). It exhibits photospheric and chromospheric magnetic activities, which have been discovered at optical (Cutispoto et al. 1995; Strassmeier 2000; Savanov & Strassmeier 2008; etc), ultra-violet (Pounds et al. 1993) and X-ray wavelengths (Voges et al. 1999).

Strassmeier et al. (2000) discovered that V1355 Ori exhibited very strong emission over the local continuum in Ca II H&K lines, and showed weak emission in one single H $\alpha$  line. Strassmeier (2000) detected a strong flare in the H $\alpha$  line during a doppler imaging observation in 1998. He also found that the H $\alpha$  profile varies with the orbital

phase during the three observing epochs in 1997, 1998 and 1999 (Strassmeier 2000). The profile of the H $\alpha$  line appears to be quite complex, ranging from an extremely strong emission due to flaring emission with a central sharp absorption to partial emission with a red absorption component, and to very narrow absorption (Strassmeier et al. 2000; Strassmeier 2000). No analysis has been carried out regarding the H $\delta$ , H $\gamma$ , H $\beta$ , Na I D<sub>1</sub>, D<sub>2</sub> and Ca II infrared triplet (IRT) lines to date.

It is of great importance to determine the behavior of chromospheric activity indicators, and chromospheric activity properties and evolution (Hall 2008; Montes et al. 2004; Zhang et al. 2015, 2016a,b; etc).

In this paper, we present new high-resolution observations of V1355 Ori. We also analyze the properties of chromospheric activity for the Ca II H&K, H $\delta$ , H $\gamma$ , H $\beta$ , Na I D<sub>1</sub>, D<sub>2</sub>, H $\alpha$  and Ca II IRT lines.

**Table 1** Observation log of V1355 Ori Using the 1.8-m and 2.4-m Telescopes

Date	HJD (245,) (d)	Exp. time (s)	S/N										
			Ca II IRT	Ca II IRT	Ca II IRT	H $\alpha$	Metal line	Na I	H $\beta$	H $\gamma$	H $\delta$	Ca II H	Ca II K
			$\lambda$ 8662	$\lambda$ 8542	$\lambda$ 8498				(4861 Å)	(4341 Å)	(4102 Å)	(3968 Å)	(3933 Å)
20150122	7045.22327	3600	58	62	52	52	81	70					
20150124	7046.23188	1800	47	51	44	44	53	51					
20150127	7050.17989	2400	45	50	43	43	54	52					
20150204	7058.14409	3600	68	73	64	64	77	73					
20150206	7060.11388	3600	67	71	62	62	81	75					
20150209	7063.11839	1800	45	49	43	43	52	47					
20150210	7064.13065	2400	49	53	45	45	58	55					
20150211	7065.09594	3600	53	56	48	48	60	55					
20150212	7066.11174	3600	57	63	54	54	68	65					
20150213	7067.12605	3600	53	57	49	49	62	57					
20150214	7068.12689	3600	58	67	55	55	76	71					
20150215	7069.07940	3600	63	66	54	54	66	61					
20160129	7417.15243	3600	87	84	63	67	89	74	28	17	10	7	6
20160226	7445.11321	3600	84	81	61	60	85	71	29	17	10	6	6
20160227	7446.07349	5400	151	145	110	107	151	125	48	30	16	10	10

## 2 OBSERVATIONS

We obtained new high-resolution spectra for V1355 Ori on 12 nights between 2015 Jan. 22 and Feb. 15 using a Coudé Echelle Spectrograph and a Tektronix CCD detector with  $2048 \times 2048$  pixels mounted on the 1.8 meter telescope (Rao et al. 2008) at Lijiang station of Yunnan Observatories. The slit width of the spectrograph on the 1.8-m telescope was  $61.7 \mu\text{m}$ . The resolution is approximately 50 000 in terms of the full width at half maximum (FWHM) of arc lines. The spectral resolution is approximately 50 000 and the spectral wavelength region is approximately 5760–11 960 Å (Zhang et al. 2016a). The limiting magnitude of the equipment is about 11.5 mag at present. In order to obtain synthesized spectra depicting the stellar photospheric contribution of V1355 Ori, we specifically chose and observed four single inactive stars (HR 617 (K1 III), Beta Gem (K0 III), HR 4182 (G9 IV) and HR 495 (K2 IV)) with spectral types and luminosity classes similar to those of V1355 Ori. HR 617 and Beta Gem were also used as reference stars for V1355 Ori to investigate chromospheric activity (Strassmeier 2000; etc).

We also observed V1355 Ori using the new high-resolution spectrograph and a Tektronix CCD detector with  $4096 \times 4096$  pixels mounted on the 2.4-m telescope (Fan et al. 2015) at Lijiang station of Yunnan Observatories on three nights (2016 Jan. 29, Feb. 26 and Feb. 27). The slit width used in this part of the observation was  $62.5 \mu\text{m}$ . The spectral wavelength region is approximately 3890–10 600 Å. The spectral resolution in terms of the FWHM of the arc comparison lines is  $0.110 \text{ Å}$  in the Ca II H&K lines,  $0.145 \text{ Å}$  in H $\delta$ ,  $0.117 \text{ Å}$  in H $\gamma$ ,  $0.152 \text{ Å}$  in H $\beta$ ,  $0.146 \text{ Å}$  in several metal lines (6400–6510 Å),  $0.147 \text{ Å}$  in He I D<sub>3</sub>, Na I D<sub>1</sub>, D<sub>2</sub> lines,  $0.150 \text{ Å}$  in the H $\alpha$  line,  $0.212 \text{ Å}$  in the Ca II IRT 8498 Å line,  $0.245 \text{ Å}$  in the Ca II IRT 8542 Å line, and  $0.227 \text{ Å}$  in the Ca II IRT 8662 Å line. The corre-

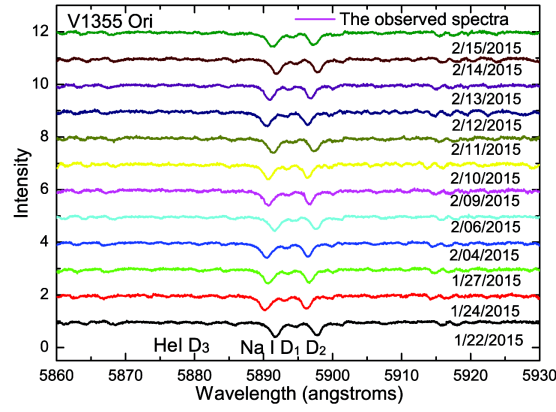
sponding spectral resolution is about 43 000 according to the FWHM of the arc comparison lines. The limiting magnitude of the equipment is about 12 mag at present. We also observed HR 617 (K1 III) as a reference star for V1355 Ori to investigate chromospheric activity.

We followed the standard process to reduce the spectra using the Image Reduction and Analysis Facility (IRAF) package, which contains tools to perform CCD image trimming, bias subtraction, flat-field correction, removal of cosmic rays, background subtraction and multi-spectrum extraction. The wavelength was calibrated using a Th-Ar lamp, and the observed spectra were normalized by a low-order polynomial function. The spectra of V1355 Ori from the Lijiang 1.8-m telescope are illustrated in Figure 1 and the spectra from the 2.4-m telescope are plotted in Figure 2. We list our observation log of V1355 Ori in Table 1, which includes observational date, the Heliocentric Julian Date (HJD), exposure time and signal to noise (S/N) ratio of the chromospherically active lines.

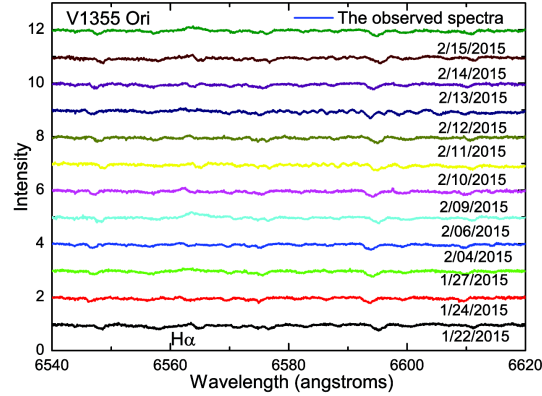
## 3 SPECTROSCOPIC ANALYSIS

For the observed spectra (Figs. 1 and 2), all the H $\alpha$  spectral lines exhibit variable behavior (filled-in absorption, partial emission with a center absorption component or emission above the continuum). The Na I lines demonstrate deep absorptions and the Ca II IRT lines exhibit filled-in absorptions with minor self-reversal core emissions. The Ca II H&K lines show obvious emissions above the continuum. The H $\delta$ , H $\gamma$  and H $\beta$  lines exhibit absorptions.

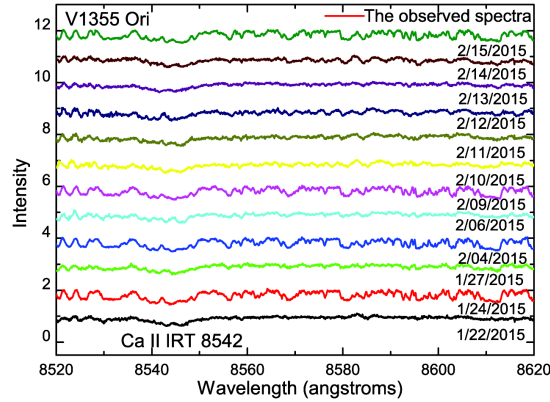
We analyzed the spectra of V1355 Ori using a synthetic spectral subtraction technique (Barden 1985; Montes et al. 1995). The synthesized spectra of V1355 Ori were obtained from rotationally broadened and radial-velocity shifted spectra of a single inactive star with similar spectral type and luminosity class as our object. The rotational ve-



(a)



(b)

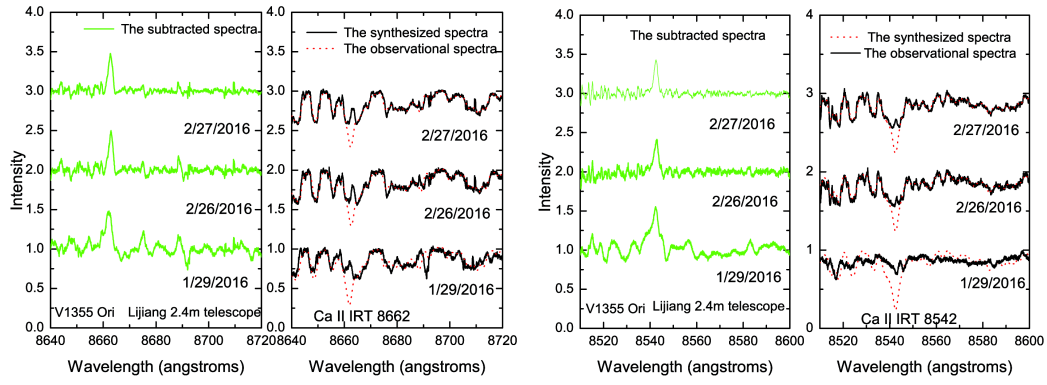


(c)

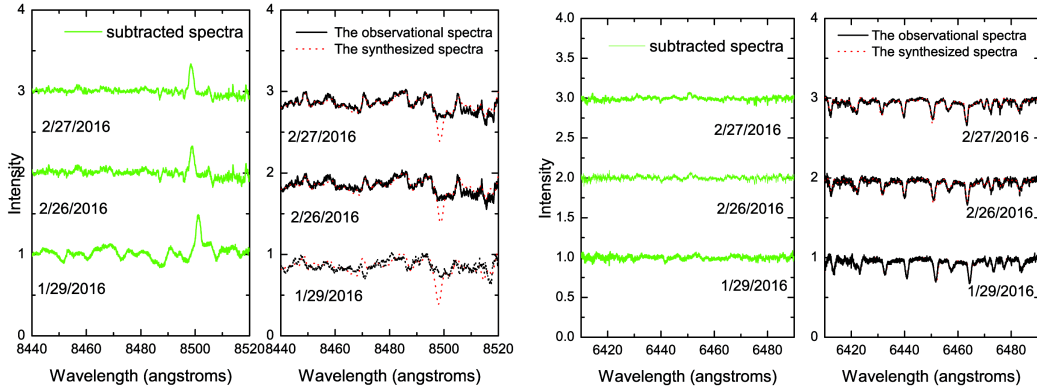
**Fig. 1** All the observed spectra for V1355 Ori using the 1.8-m telescope in the He I D<sub>3</sub>, Na I D<sub>1</sub>, D<sub>2</sub>, H $\alpha$  and Ca II 8542 lines are shown. All these spectra are vertically shifted by 1.

locity ( $v \sin i = 39.6 \text{ km s}^{-1}$ ) of V1355 Ori was determined using some single metallic spectral lines in the wavelength ranges of 6387–6487 Å (Fig. 2). We chose Beta Gem for the 1.8-m telescope and HR 617 for the 2.4-m telescope for this purpose. Our result is similar to the previous results of  $40 \pm 0.5 \text{ km s}^{-1}$  derived by Strassmeier (2000) and  $46 \text{ km s}^{-1}$  (Osten & Saar 1998; Strassmeier et al. 1999). All the subtracted, observed and synthesized spec-

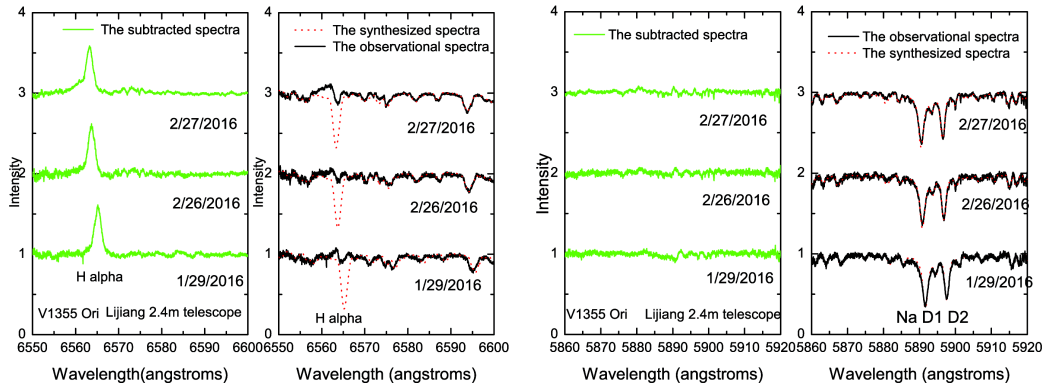
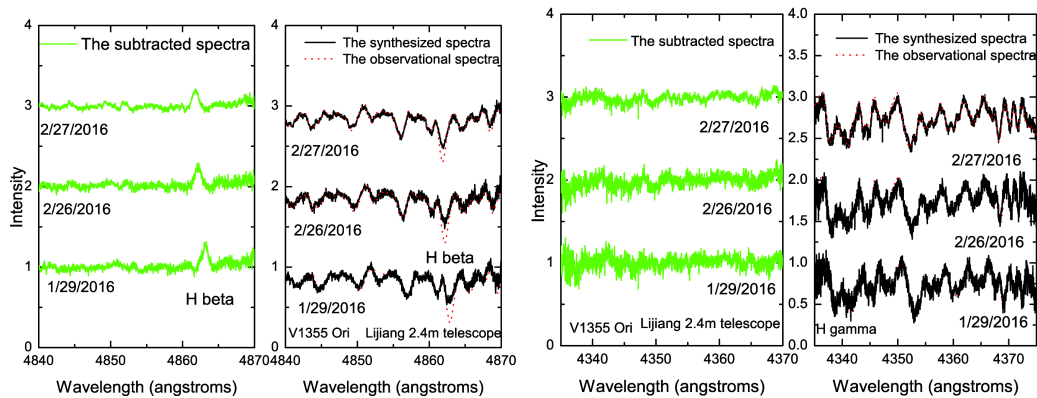
tra are shown in Figures 2 and 3. The Ca II IRT lines have a poorer quality than the Na I and H $\alpha$  lines because of shorter exposure time and poorer weather conditions at the time of observation. For Ca II H&K lines, we did not use a spectral subtraction technique to analyze them because of their emission above continuum and low S/N. The subtraction spectra of the Na I D<sub>1</sub>, D<sub>2</sub> lines show weak emissions, but all subtracted spectra with the H $\alpha$  line exhibit



(a) Ca II 8662 and 8542 lines



(b) Ca II 8498 and metal lines

(c) H $\alpha$  and Na I D<sub>1</sub>, D<sub>2</sub> lines(d) H $\beta$  and H $\gamma$

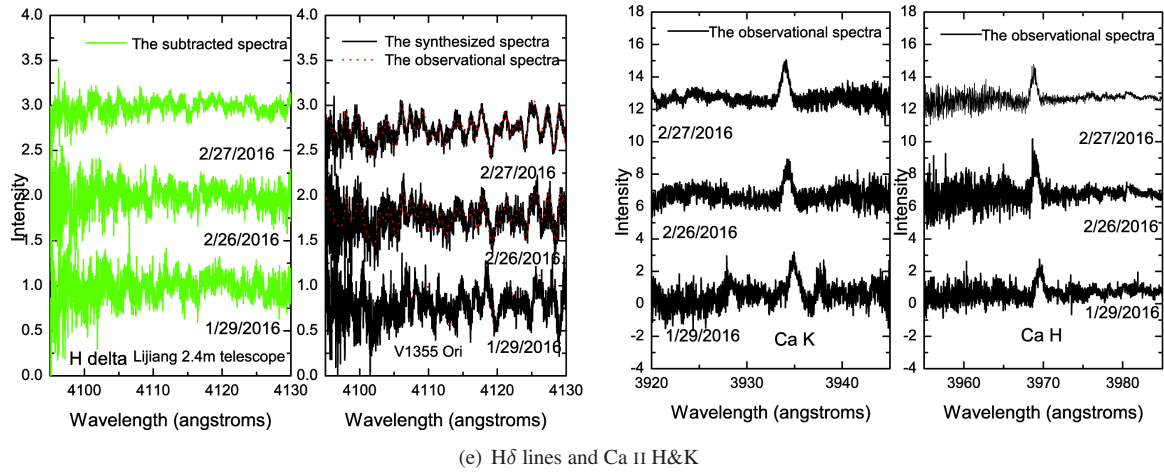


**Fig. 2** The observed, synthesized and subtracted spectra of V1355 Ori from the 2.4-m telescope in several spectral lines (Ca II H&K, H $\delta$ , H $\gamma$ , H $\beta$ , Na I D<sub>1</sub>, D<sub>2</sub>, H $\alpha$  and Ca II IRT lines), and metal lines in the spectral wavelength region of 6400–6500 Å. All these spectra were vertically shifted by several units.

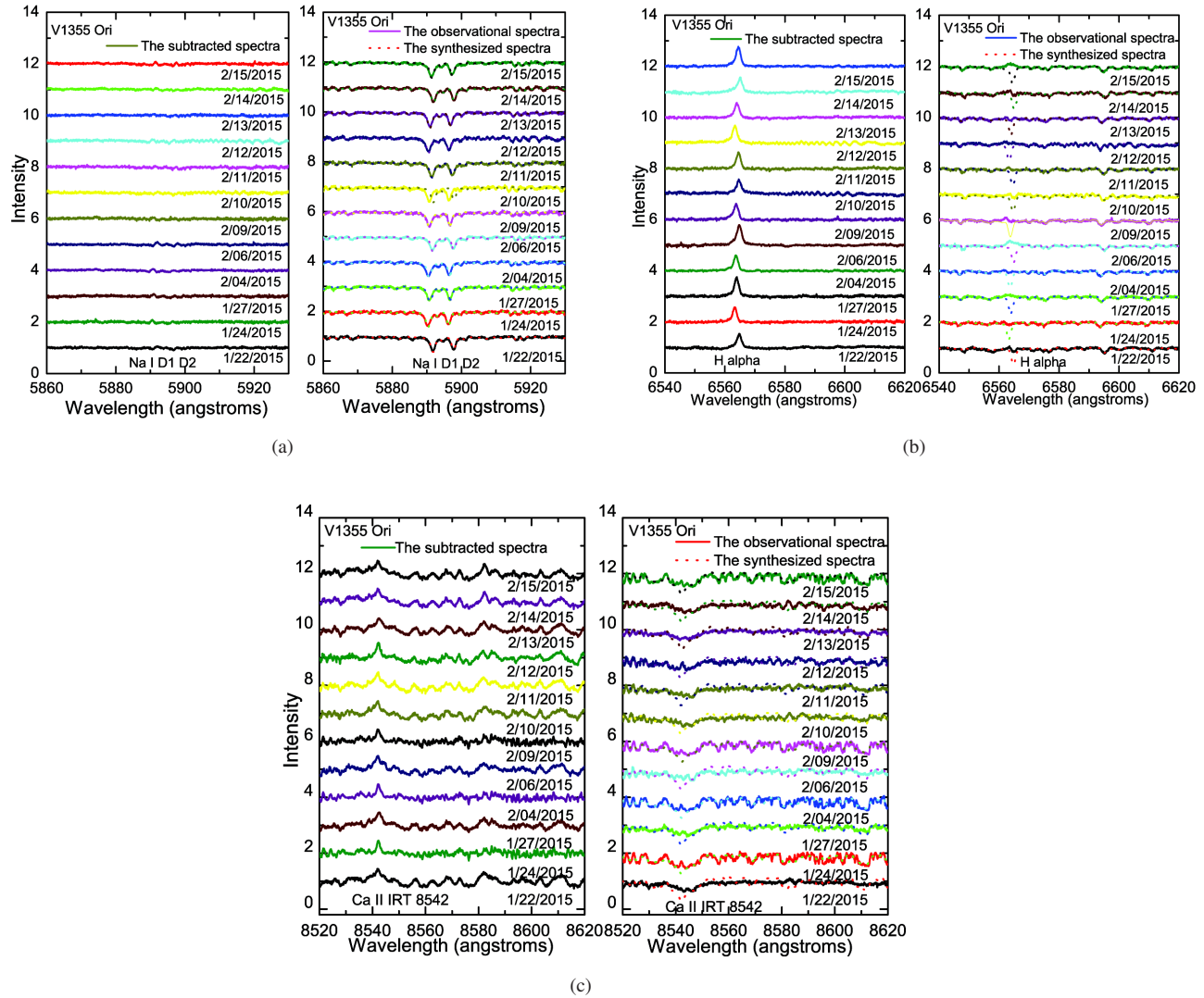


**Fig. 3** Observed and synthesized (*right*), and subtracted (*left*) spectra of V1355 Ori using the 1.8-m telescope.



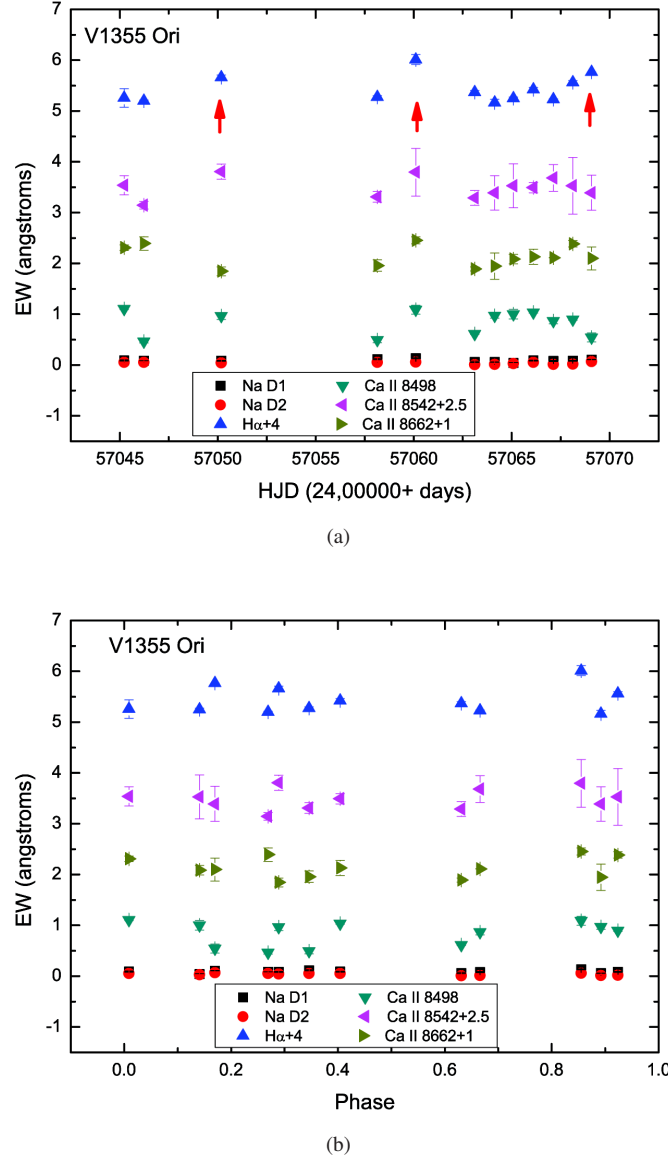


**Fig. 4** EW light curves of chromospheric excess emissions of V1355 Ori vs. HJD (a) and the orbital phases (b). Red arrows mark the events where EWs increased significantly.

obvious emission over the continuum. The excess spectra for the Ca II IRT lines display emissions. There are no excess emissions in the H $\delta$  and H $\gamma$  lines, but there is excess emission in the H $\beta$  line. The EWs were calculated by integrating them above the emission lines using the SPLOT package in IRAF. The methods for calculating the EWs and their uncertainties have been published in our previous papers (Zhang & Gu 2008; Zhang et al. 2014, 2015; etc). For V1355 Ori, the uncertainties in the EWs are underestimated because the S/N values for these spectra are low and we do not consider the effect of error in the continuum.

The values of the HJD, orbital phase, the excess EWs of chromospheric activity indicators, and the ratios of  $EW_{8542}/EW_{8498}$  and  $E_{H\alpha}/E_{H\beta}$  are listed in Table 2. The orbital phases were calculated using the function:  $HJD =$

$2450540.365 + 3.87192 \times E$  (Strassmeier 2000). We also plotted the EWs of V1355 Ori versus HJD and phase in Figure 4, where different symbols represent different chromospheric activity indicators.

#### 4 DISCUSSIONS AND CONCLUSIONS

The spectra that we observed show obvious emissions above continuum in the Ca II H&K lines, and variable behavior in the H $\alpha$  line. Our results further confirm this type of behavior observed in the Ca II H&K lines (Strassmeier et al. 2000) and the H $\alpha$  line (Strassmeier 2000; Strassmeier et al. 2000). These spectra show deep absorptions in the Na I D<sub>1</sub>, D<sub>2</sub> lines, absorptions in the H $\delta$ , H $\gamma$  and H $\beta$ , and minor self-reversal emissions in the Ca II IRT absorp-

**Table 2** The Values of Chromospheric Emissions from V1355 Ori

HJD(245.)	Phase	EW <sub>CaII K</sub> (Å)	EW <sub>CaII H</sub> (Å)	EW <sub>NaID1</sub> (Å)	EW <sub>NaID2</sub> (Å)	EW <sub>Hα</sub> (Å)	EW <sub>Hβ</sub> (Å)	E <sub>Hα</sub> /E <sub>Hβ</sub>	EW <sub>CaII 8498</sub> (Å)	EW <sub>CaII 8542</sub> (Å)	EW <sub>CaII 8662</sub> (Å)	EW <sub>8542</sub> /EW <sub>8498</sub>
7045.22327	0.009	-	-	0.093 ± 0.011	0.055 ± 0.010	1.257 ± 0.180	-	-	1.107 ± 0.016	1.037 ± 0.189	1.31 ± 0.057	0.937 ± 0.154
7046.23188	0.269	-	-	0.087 ± 0.002	0.058 ± 0.010	1.200 ± 0.016	-	-	0.464 ± 0.029	0.646 ± 0.076	1.393 ± 0.133	1.392 ± 0.132
7050.17989	0.289	-	-	0.086 ± 0.008	0.049 ± 0.001	1.663 ± 0.043	-	-	0.967 ± 0.070	1.306 ± 0.148	0.846 ± 0.086	1.351 ± 0.113
7058.14409	0.346	-	-	0.115 ± 0.009	0.057 ± 0.009	1.276 ± 0.023	-	-	0.496 ± 0.055	0.810 ± 0.106	0.959 ± 0.11	1.633 ± 0.172
7060.11388	0.855	-	-	0.137 ± 0.011	0.063 ± 0.001	2.012 ± 0.098	-	-	1.089 ± 0.087	1.295 ± 0.470	1.455 ± 0.069	1.189 ± 0.375
7063.11839	0.631	-	-	0.063 ± 0.013	0.011 ± 0.005	1.371 ± 0.034	-	-	0.614 ± 0.009	0.791 ± 0.144	0.891 ± 0.039	1.288 ± 0.226
7064.13065	0.892	-	-	0.061 ± 0.002	0.016 ± 0.012	1.163 ± 0.064	-	-	0.971 ± 0.047	0.890 ± 0.338	0.945 ± 0.259	0.917 ± 0.290
7065.09594	0.141	-	-	0.043 ± 0.003	0.032 ± 0.007	1.249 ± 0.025	-	-	1.003 ± 0.094	1.028 ± 0.431	1.086 ± 0.095	1.025 ± 0.340
7066.11174	0.404	-	-	0.090 ± 0.009	0.056 ± 0.005	1.425 ± 0.038	-	-	1.039 ± 0.015	0.992 ± 0.102	1.131 ± 0.149	0.954 ± 0.082
7067.12605	0.666	-	-	0.082 ± 0.008	0.017 ± 0.001	1.227 ± 0.011	-	-	0.869 ± 0.058	1.183 ± 0.262	1.113 ± 0.003	1.361 ± 0.265
7068.12689	0.924	-	-	0.086 ± 0.008	0.023 ± 0.001	1.561 ± 0.034	-	-	0.896 ± 0.014	1.028 ± 0.555	1.386 ± 0.062	1.147 ± 0.608
7069.07940	0.170	-	-	0.108 ± 0.003	0.073 ± 0.005	1.765 ± 0.003	-	-	0.544 ± 0.090	0.891 ± 0.347	1.099 ± 0.228	1.638 ± 0.576
7417.15243	0.593	3.992±0.279	4.261 ± 0.167	-	-	1.255 ± 0.056	0.273 ± 0.010	5.789 ± 0.046	1.054 ± 0.141	1.619 ± 0.091	1.271 ± 0.252	1.536 ± 0.119
7445.11321	0.288	3.608 ± 0.092	2.620 ± 0.230	-	-	1.232 ± 0.030	0.267 ± 0.007	5.811 ± 0.011	0.605 ± 0.024	0.869 ± 0.093	0.926 ± 0.012	1.436 ± 0.097
7446.07349	0.536	4.214 ± 0.160	3.834 ± 0.091	-	-	1.546 ± 0.100	0.235 ± 0.005	8.285 ± 0.360	0.614 ± 0.018	0.872 ± 0.038	0.960 ± 0.020	1.420 ± 0.020

tion lines. These features further demonstrate the chromospheric activity of V1355 Ori. The subtracted spectra exhibit no excess emission in the H $\delta$  or H $\gamma$  lines, trace amounts of emission in the Na I lines, excess emission in the H $\beta$  line, clear emission in the H $\alpha$  line and weak excess emissions in the Ca II IRT lines. The maximum EW of our H $\alpha$  line is smaller than that of the large H $\alpha$  flare at HJD 2450909.6 (Strassmeier 2000).

The value of the ratio (EW<sub>8542</sub>/EW<sub>8498</sub>) is also an indicator of chromospheric activity. For V1355 Ori, the value of EW<sub>8542</sub>/EW<sub>8498</sub> is in the range 0.9–1.7. Smaller values indicate optically thick emissions from a possible stellar plage event. These values are also consistent with other behaviors of chromospheric activity indicators. Similar values were also discovered in many chromospherically active stars (Cao & Gu 2015; Arévalo & Lázaro 1999; Gu et al. 2002; Montes et al. 2001; Zhang et al. 2014, 2015, 2016a; etc).

We calculated the ratio of  $E_{H\alpha}/E_{H\beta}$  for V1355 Ori in our 2016 run (Table 2). The ratio of excess emission  $E_{H\alpha}/E_{H\beta}$  was corrected with the function  $\frac{E_{H\alpha}}{E_{H\beta}} = \frac{EW_{H\alpha}}{EW_{H\beta}} \times 0.2444 \times 2.512^{(B-R)}$  from Hall & Ramsey (1992). The color index of V1355 Ori ( $B - R$ ) = 1.78 was assumed from its spectral type. Buzasi (1989) concluded that low ratios (1–2) can be achieved both in plages and prominences viewed against the disk, but high values (3–15) can only be achieved in prominence-like structures viewed off the stellar limb. We obtained a mean value of  $6.628 \pm 0.139$  for  $E_{H\alpha}/E_{H\beta}$  for V1355 Ori. The ratio  $E_{H\alpha}/E_{H\beta} (\gtrsim 3)$  implies that the emission of Balmer lines originates from prominence-like material (Buzasi 1989; Hall & Ramsey 1992).

It is unpractical for us to carry out a detailed study of the chromospheric rotational modulation of V1355 Ori because of limitations in data acquisition during a night (we normally only had a partial night) and the total time span required. We had 22 nights to use the 1.8-m telescope for studying V1355 Ori, which correspond to approximately six orbital periods. Our results do not show

any obvious phase modulations in all the chromospheric activity indicator lines (Fig. 4). Chromospheric intensity as well as the presence of circumstellar material may dilute or even suppress the rotationally modulated plage signature (Strassmeier 2000). As illustrated in Figure 4, there is a weak time-variation of excess emission EWs in the Na I D<sub>1</sub>, D<sub>2</sub>, Ca II IRT and H $\alpha$  (which is the strongest) lines. The increase in EWs is marked by red arrows in Figure 4. All these indicators are consistent with each other. These phenomena can be explained by plage events, which are consistent with the observed behavior of these chromospheric activity indicators. In the future, further high-resolution spectra will be required to study the chromospheric activity cycle of V1355 Ori, such as those of the photospheric cycle reported by Savanov & Strassmeier (2008).

**Acknowledgements** This work was supported by the Astronomic Joint Fund of the National Natural Science Foundation of China and Chinese Academy of Sciences (U1431114, U1631236, U1631109 and 11263001), and science and technology innovation team of Guizhou province (No. 20154017). This work was also supported by the Natural Science Foundation of Guizhou Province Office of Education (Grant No. 2014298). We acknowledge the support of staff at the Lijiang 2.4 m telescope. Funding for the telescope was provided by CAS and the People’s Government of Yunnan Province.

## References

- Arévalo, M. J., & Lázaro, C. 1999, *AJ*, 118, 1015
- Barden, S. C. 1985, *ApJ*, 295, 162
- Buzasi, D. L. 1989, *A Study of Active Regions on RS CVn Stars*, PhD Thesis, Pennsylvania State University, University Park
- Cao, D., & Gu, S. 2015, *MNRAS*, 449, 1380
- Cutispoto, G., Pallavicini, R., Kuerster, M., & Rodono, M. 1995, *A&A*, 297, 764
- Eker, Z., Ak, N. F., Bilir, S., et al. 2008, *MNRAS*, 389, 1722

- Fan, Y. F., Bai, J. M., Zhang, J. J., et al. 2015, RAA (Research in Astronomy and Astrophysics), 15, 918
- Gu, S.-H., Tan, H.-S., Shan, H.-G., & Zhang, F.-H. 2002, A&A, 388, 889
- Hall, J. C., & Ramsey, L. W. 1992, AJ, 104, 1942
- Hall, J. C. 2008, Living Reviews in Solar Physics, 5
- Montes, D., Fernandez-Figueroa, M. J., de Castro, E., & Cornide, M. 1995, A&AS, 109, 135
- Montes, D., López-Santiago, J., Gálvez, M. C., et al. 2001, MNRAS, 328, 45
- Montes, D., Crespo-Chacón, I., Gálvez, M. C., et al. 2004, Lecture Notes and Essays in Astrophysics, 1, 119
- Osten, R. A., & Saar, S. H. 1998, MNRAS, 295, 257
- Pounds, K. A., Allan, D. J., Barber, C., et al. 1993, MNRAS, 260, 77
- Rao, C., Jiang, W., Zhang, Y., et al. 2008, in Proc. SPIE, 7015, Adaptive Optics Systems, 70155Y
- Savanov, I. S., & Strassmeier, K. G. 2008, Astronomische Nachrichten, 329, 364
- Strassmeier, K. G., Serkowitsch, E., & Granzer, T. 1999, A&AS, 140, 29
- Strassmeier, K. G. 2000, A&A, 357, 608
- Strassmeier, K., Washuettl, A., Granzer, T., Scheck, M., & Weber, M. 2000, A&AS, 142, 275
- Voges, W., Aschenbach, B., Boller, T., et al. 1999, A&A, 349, 389
- Zhang, L.-Y., & Gu, S.-H. 2008, A&A, 487, 709
- Zhang, L., Pi, Q., Zhu, Z., Zhang, X., & Li, Z. 2014, New Astron., 32, 1
- Zhang, L.-Y., Pi, Q.-F., & Zhu, Z.-Z. 2015, RAA (Research in Astronomy and Astrophysics), 15, 252
- Zhang, L., Pi, Q., Han, X. L., Chang, L., & Wang, D. 2016a, MNRAS, 459, 854
- Zhang, L., Pi, Q., Han, X. L., et al. 2016b, New Astron., 44, 66